Journal of Macromolecular Science, Part A
Publication details, including instructions for authors and subscription information:
http://www.informaworld.com/smpp/title~content=t713597274

Tetraphenylethane Iniferters. 3. "Living" Radical Polymerization of Methyl Methacrylate Using Toluene-Diisocyanate-Based Polyurethane Iniferter

K. Tharanikkarasu[a]; Ganga Radhakrishnan[a]
[a] Polymer Division Central Leather Research Institute Adyar, Madras, India

To cite this Article Tharanikkarasu, K. and Radhakrishnan, Ganga(1996) 'Tetraphenylethane Iniferters. 3. "Living" Radical Polymerization of Methyl Methacrylate Using Toluene-Diisocyanate-Based Polyurethane Iniferter', Journal of Macromolecular Science, Part A, 33: 4, 417 — 437
To link to this Article: DOI: 10.1080/10601329608010868
URL: http://dx.doi.org/10.1080/10601329608010868

J.M.S.—PURE APPL. CHEM., A33(4), pp. 417–437 (1996)

TETRAPHENYLETHANE INIFERTERS. 3. "LIVING" RADICAL POLYMERIZATION OF METHYL METHACRYLATE USING TOLUENE-DIISOCYANATE-BASED POLYURETHANE INIFERTER

K. THARANIKKARASU and GANGA RADHAKRISHNAN*

Polymer Division
Central Leather Research Institute
Adyar, Madras 600020, India

ABSTRACT

Polyurethane iniferter, synthesized from toluene diisocyanate and 1,1,2,2-tetraphenyl-1,2-ethanediol, was used to polymerize methyl methacrylate. The rate equation and overall activation energy have been determined from the kinetic results. The number-average molecular weight of the polymethyl methacrylate increased while increasing both conversion and polymerization time. Bimodal molecular weight distribution was observed in gel permeation chromatography. Molecular weight build up occurs when the postpolymerization of polymethyl methacrylate was carried out. It is hence inferred that polyurethane iniferter acts as a thermal iniferter and follows "living" radical polymerization. Polymethyl methacrylate prepared with the polyurethane iniferter initiates the polymerization of styrene to yield polymethyl methacrylate-polystyrene block copolymers by a subsequent supply of thermal energy.

INTRODUCTION

The chemoselectivity of the polymerization method decides the molecular weight, molecular weight distribution (MWD), end groups, etc. of the resulting polymer. Even though radical polymerization is less chemoselective when compared to ionic polymerization methods, it is widely used in industry due to the ease of

processing and its suitability to polymerize polar monomers and less rigorous polymerization conditions.

Iniferters

In order to improve the chemoselectivity of radical polymerization, Otsu and coworkers proposed the concept of iniferter [1] and a model for living radical polymerization [2]. Iniferter is an *ini*tiator, trans*fer* agent, and/or *ter*minator for free radical polymerization. It avoids ordinary bimolecular terminations and undergoes initiation, chain transfer to the initiator, and/or primary radical termination. Hence the number of iniferter fragments per one polymer chain is always 2 [1, 2, 6, 7]. This type of radical polymerization may simply be considered as an insertion of monomer (M) molecules into an iniferter (I—I) as given in Eq. (1):

$$\text{I—I} + n\text{M} \longrightarrow \text{I}\{\text{M}\}_n\text{I} \tag{1}$$

Some organic sulfur compounds [2–6], phenylazotriphenylmethane [2, 7], azobisdiphenyl methane [8], tetraphenylethane derivatives [9, 10], and thiuram disulfides [11–13] served as iniferters for the polymerization of vinyl monomers. The quantitative theory of kinetics for iniferter polymerization was reported recently [14].

"Living" Radical Polymerization

Living polymerization should have high chemoselectivity to synthesize well-defined polymers. The criteria of livingness is not well defined but it is stressed that the chain-breaking reactions such as bimolecular irreversible termination in radical polymerization or transfer reaction in cationic polymerization should not occur at the time of complete conversion of monomer molecules. If the bimolecular irreversible termination is >5% at 99% of monomer conversion, then the system is called "living" radical polymerization (here the quotation marks denote the presence of bimolecular irreversible termination) [15].

A typical synthesis of well-defined polymers by radical polymerization requires a low concentration of free radicals and a relatively shorter chain length. Even though these two prerequisites are contradictory, they can be achieved by the reversible deactivation of growing free radicals. There are three possibilities to deactivate growing free radicals [15]. In the first case, activation takes place by the cleavage of P_n—I into a growing polymer radical, $P_n^{\cdot}$, and a scavenging radical, $I^{\cdot}$. Here $P_n^{\cdot}$ is responsible for the propagation with monomer molecules and $I^{\cdot}$ is responsible for reversible deactivation. The scavenger $I^{\cdot}$ can react only with $P_n^{\cdot}$ but not with monomer molecules as given in Eq. (2):

$$\underset{\text{(A)}}{P_n\text{—I}} \rightleftharpoons \underset{\text{(B)}}{P_n^{\cdot}} + \underset{\text{(C)}}{I^{\cdot}} \xrightarrow{x\text{P}} \underset{\text{(D)}}{P_{n+x}\text{—I}}$$

$$\text{D} \rightleftharpoons P_{n+x}^{\cdot} + I^{\cdot} \xrightarrow{y\text{P}} P_{n+x+y}\text{—I} \longrightarrow \cdots \tag{2}$$

Iniferters which follow "living" radical polymerization fall under this case [2–8]. If a scavenger of growing radical acts as a neutral species, a persistent radical,

$\{P-R\}^{\cdot}$, with an odd number of electron, will be reversibly formed as given in Eq. (3):

$$\{P_n-R\}^{\cdot} \rightleftharpoons P_n^{\cdot} + R \xrightarrow{x\mathrm{P}} \{P_{n+x}-R\}^{\cdot}$$

$$\{P_{n+x}-R\}^{\cdot} \rightleftharpoons P_{n+x}^{\cdot} + R \xrightarrow{y\mathrm{P}} \{P_{n+x+y}-R\}^{\cdot} \longrightarrow \cdots \qquad (3)$$

Here also $P_n^{\cdot}$ is responsible for polymerization and R is responsible for reversible deactivation. This is the second case of "living" radical polymerization, and the kinetic requirements are identical to case I. The "aged" chromium(II) acetate–benzoyl peroxide system [16] and the triisobutylaluminum-2,2′-bipyridyl-2,2,6,6-tetramethyl-1-piperidinyloxy system [17, 18] fall in this case. In the third case, a growing radical, $P_n^{\cdot}$, reacts rapidly and selectively with a transfer agent, P_1-S, to exchange the S and forms a dormant species, P_n-S, as well as a new radical, $P_1^{\cdot}$, as given in Eq. (4):

$$\begin{array}{ccccc} P_n^{\cdot} & + & P_1-S & \rightleftharpoons & P_n-S + P_1^{\cdot} \\ & & \downarrow \mathrm{P} & & \downarrow \mathrm{P} \\ P_n-P^{\cdot} & + & P_1-P-S & \rightleftharpoons & P_n-P-S + P_1-P^{\cdot} \\ & & \downarrow & & \downarrow \\ & & \vdots & & \vdots \end{array} \qquad (4)$$

Here the concentration of transfer agents has to be kept low enough to reduce the possibility of bimolecular termination. Radical polymerizations using degenerative transfer agents such as alkoxyamines [19] and alkyl iodides [20] are examples of this case. The concept of reversible deactivation of growing polymer radicals was recently used in the controlled radical polymerization of vinyl monomers [21].

Macroinitiators

Polymers which consist of initiating groups such as azo, peroxy, disulfide, etc. in the main or side chain are called macroinitiators. In macroinitiators, the initiating groups can be introduced (a) at one end of each polymer chain, (b) at both ends of each polymer chain, (c) between polymer blocks, (d) as side chains, and (e) between organic moieties in the polymer. When these five types are decomposed in the presence of vinyl monomers, diblock, triblock, multiblock, graft copolymers, and homopolymers are formed, respectively.

One of the advantages in "living" radical polymerization using iniferters is that the Trommsdorff effect does not occur because radicals formed during bulk polymerization are mostly consumed by a scavenger through primary radical termination [15]. Polymers can be synthesized even above the ceiling temperature using iniferters [9]. Simple evidence for living radical polymerization is that the molecular weight of the polymer produced increases with both increasing polymerization time and conversion [2–8].

Hexa- and tetraphenylethane derivatives are capable of acting as iniferters and of following "living" radical polymerization [22]. These compounds generate radicals through homolytic cleavage of their central ethane bond [23, 24]. Silicone-based macroinitiators which consist of tetraphenylethane groups in their main chain

have been used to synthesize silicone–vinyl block copolymers [25, 26]. 1,1,2,2-Tetraphenyl-1,2-ethanediol (TPED) is a well-known free-radical initiator [27] but it neither serves as an iniferter nor proceeds via living radical polymerization even though it contains a well-known iniferter group (tetraphenylethane) in its structure. In order to use this iniferter group for living radical polymerization, a novel polyurethane macroiniferter (BPT) has been synthesized by reacting TPED with toluene diisocyanate (TDI) [28]. After reacting —OH groups of TPED with TDI, the resulting BPT proceeds via a "living" radical polymerization mechanism in the polymerization of acrylonitrile [29]. The polymerization of methyl methacrylate (MMA) with BPT and postpolymerization of the resulting polymethyl methacrylate (PMMA) are reported in this paper.

EXPERIMENTAL SECTION

Materials

TDI (a mixture of 80% 2,4 and 20% 2,6 isomers) and dibutyltin dilaurate (DBTDL) were used as received from Aldrich, USA. Analytical grades styrene (ST) and MMA were distilled at reduced pressure after removal of inhibitor; the middle portions were stored at 0–4°C prior to use. Analytical grade *N,N*-dimethylformamide (DMF) was distilled at reduced pressure, and the middle portion was used after storage over molecular sieves (type 4A). The other reagents were of analytical grade and used as received.

Synthesis of TPED and BPT

TPED was prepared from benzophenone and propane-2-ol using the known method [30]. BPT was synthesized from TDI and TPED as reported earlier by us [28].

Kinetics

Kinetic measurements were performed using the gravimetric method. Initial rates were considered in the rate of polymerization (R_p) calculations. All rates were determined using time–conversion plots. For kinetic studies, required amounts of MMA, BPT [31], and DMF were charged into cylindrical Pyrex tubes, degassed by three alternate freeze–pump–thaw cycles, sealed under vacuum, and placed in a thermostated shaking water bath controlled to ±0.01°C for selected times. The tubes were then removed from the water bath after stipulated times and the reactions were arrested by dipping in an ice–salt mixture. The resulting PMMA solutions were poured into excess distilled water and the precipitates were filtered, using sintered-glass crucibles, washed with methanol to remove unreacted BPT, dried in vacuum, and weighed.

The same procedure was also adopted in the postpolymerization stage, but the contents used were PMMA, DMF, and MMA or ST. Distilled water and methanol were used as nonsolvents for the postpolymerized PMMA and PMMA–PST block copolymers, respectively. Acetonitrile and cyclohexane were used to extract homo-PMMA and homo-PST, respectively, from the block copolymers.

Characterization

Number-average ($\overline{M}_n$) and weight-average ($\overline{M}_w$) molecular weights and MWDs ($\overline{M}_w/\overline{M}_n$) were determined by gel permeation chromatography (GPC) using a Waters liquid chromatograph equipped with a 410 differential refractometer (RI detector) and four μ-Styragel columns (10^6, 10^5, 10^4, and 10^3Å) in series. DMF (0.01% LiBr added) was used as an eluent at a flow rate of 1.0 mL/min, and molecular weight calibrations were done using polystyrene standards. The concentration and volume of polymer solutions injected were kept constant to enable comparison of the GPC curves at different polymerization times. The Fourier transform infrared (FT-IR) spectra were recorded as a KBr pellet on a Nicolet Impact 400 FT-IR spectrophotometer. The Fourier transform nuclear magnetic resonance (FT-NMR) spectrum of PMMA-PST block copolymer was recorded on a Bruker MSL 300 MHz NMR instrument using deuterated dimethylsulfoxide as the solvent and tetramethylsilane as the internal standard. Differential scanning calorimetry (DSC) was carried out with a DuPont 910 DSC instrument at a heating rate of 10°C/min, and thermogravimetric analysis (TGA) was carried out using a DuPont 951 TGA instrument at a heating rate of 20°C/min under N_2 atmosphere.

RESULTS AND DISCUSSION

TPED consists of a tetraphenylethane group, a well-known iniferter group, in its structure, but it does not act as an iniferter or follow "living" radical polymerization in the polymerization of vinyl monomers due to the formation of benzophenone and monomer free radical in the initiation step [27, 32] as shown in Scheme 1. However, tetraphenylethane derivatives such as 1,1,2,2-tetraphenyl-1,2-dicyanoethane [11, 33, 34], 1,1,2,2-tetraphenyl-1,2-diphenoxy ethane [33, 34], 1,1,2,2-tetra-

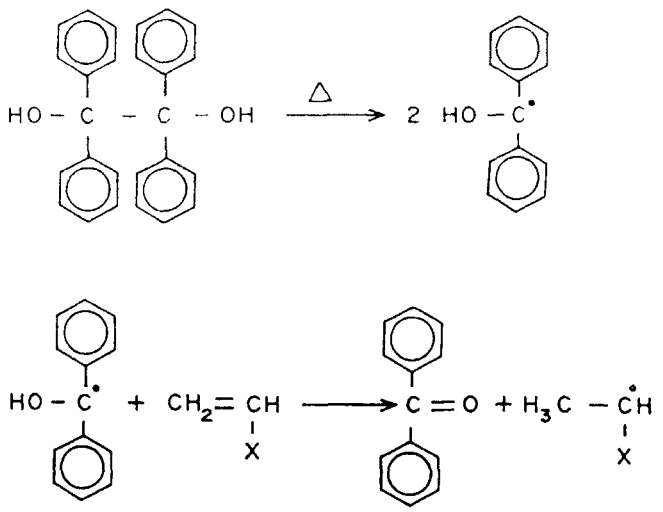

SCHEME 1.

phenyl-1,2-bis(trimethylsiloxy) ethane [33], etc. act as iniferters and follow "living" radical polymerization. If the —OH groups of TPED are modified, then it can act similar to other tetraphenylethane derivatives [11, 33, 34]. To achieve this, TPED was reacted with TDI [28], and it was found that the resulting BPT acted as a macroiniferter as well as follows "living" radical polymerization when acrylonitrile was polymerized [29]. In this article the polymerization of MMA by BPT and the synthesis of PMMA–polystyrene (PST) block copolymers are reported.

Scheme 2 explains the synthetic route, the structure of BPT, and the resulting structure of PMMA obtained from MMA and BPT. Scheme 2 also explains the possible mechanism in the "living" radical polymerization of MMA polymerization using BPT in analogy with Eq. (2) and the synthetic route as well as the structure of PMMA–PST block copolymer. Since BPT consists of initiating groups between organic moieties, as described earlier (type e), the resulting PMMA from BPT (hereinafter denoted PMMA–BPT) is a homopolymer, and PMMA–BPT forms PMMA–PST block copolymer in the presence of ST.

Kinetic Studies

In order to understand the mechanism and rates of polymerization, basic kinetic studies have been carried out by changing the temperature and BPT and MMA concentrations. The internal orders in monomer at different temperatures have been determined. Figure 1 shows time–conversion plots for MMA polymerization with BPT at different temperatures ranging from 65 to 80°C. Since BPT involves initiation, transfer reaction, and/or primary radical termination, the rates are lower than those of the conventional system [35]. Table 1 gives the results of MMA polymerization with BPT at 70°C. Figure 2 shows the time–$\ln([M]_0/[M])$ kinetic plots obtained for MMA polymerization at different temperatures. The straight lines indicate first-order kinetics with respect to monomer. Thus, monomer is involved in the rate-limiting step. The straight lines also support the steady concentration of the active species. This result reveals that the proportion of irreversible termination is low. From the Arrhenius plot of log R_p vs $1/T$ (Fig. 3), the overall activation energy, E_a, is found to be 57.4 kJ/mol, which is comparable to the overall activation energy for the polymerization of MMA using 1,1,2,2-tetraphenyl cyclopentane (64.4 ± 2.9 kJ/mol) [36].

Figure 4 shows a plot of log R_p vs log [MMA], which has a straight line with a slope of 1.2. A straight line with a slope of 0.95 is obtained in a plot of log R_p vs log[BPT] (Fig. 5). Therefore, the rate equation for the polymerization of MMA with BPT may be given as $R_p = k[BPT]^{0.95}[MMA]^{1.2}$. When compared to the reported [35] rate equation for MMA polymerization by AIBN ($R_p = k[AIBN]^{0.5}[MMA]$), the dependence of R_p on MMA concentration is almost the same. The first order of initiator concentration indicates that the proportion of irreversible termination is small. If the irreversible termination is small (< 5%), then the resulting polymer can easily be deactivated, thereby the system will follow "living" radical polymerization [15, 17, 18]. Time–conversion and time–$\overline{M}_n$ relations are shown in Fig. 6. Both conversion and $\overline{M}_n$ increase when the polymerization time increases. As explained already [1–8], these are typical results for "living" radical polymerization.

In "living" radical polymerizations for a single homopolymer, unimodal [37, 38] or bimodal [7, 11, 39] peaks were observed in GPC. When the iniferter reacts

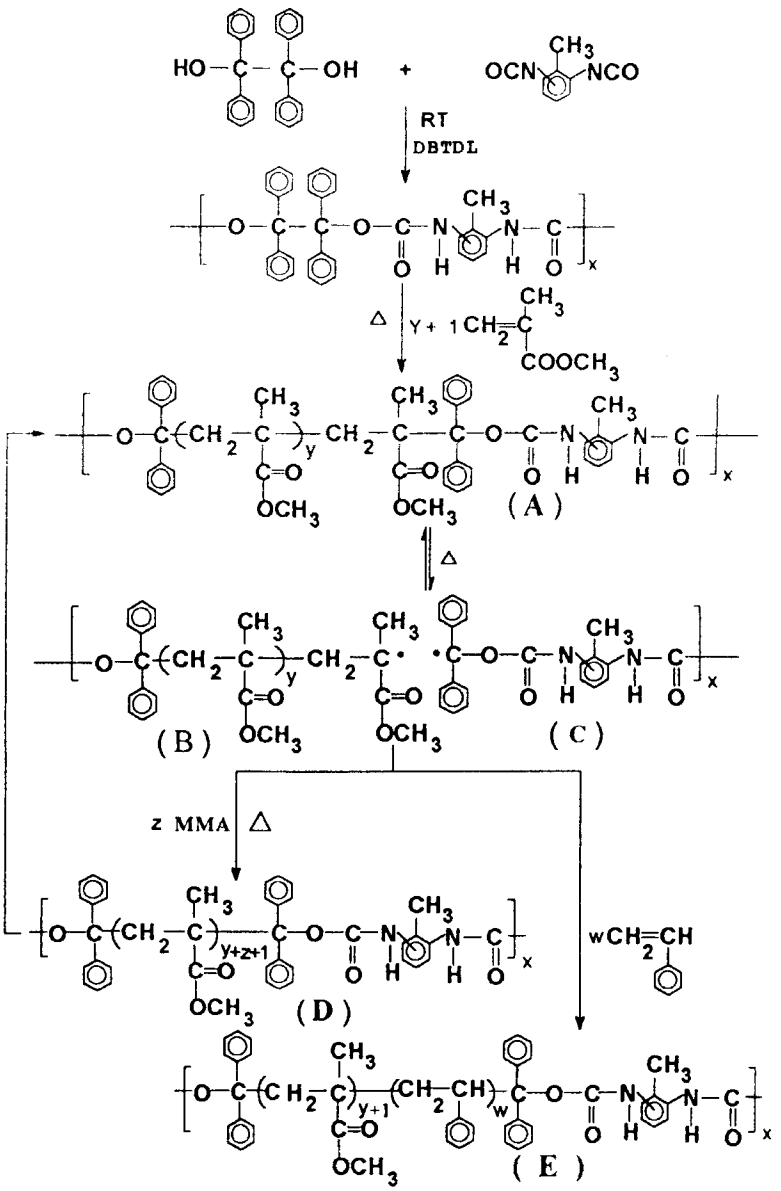

SCHEME 2.

with the monomer, the low molecular weight portions are first formed (A in Eq. 2 and Scheme 2) due to primary radical termination. As time increases, the low molecular weight portions cleave into a more reactive propagated radical (fragment B in Eq. 2 and Scheme 2) and a scavenging radical (fragment C in Eq. 2 and Scheme 2). When fragments B react further with the same monomer molecules, then a high molecular weight polymer is obtained (fragment D in Eq. 2 and Scheme 2). When the difference in molecular weight between these two fractions (between A and D)

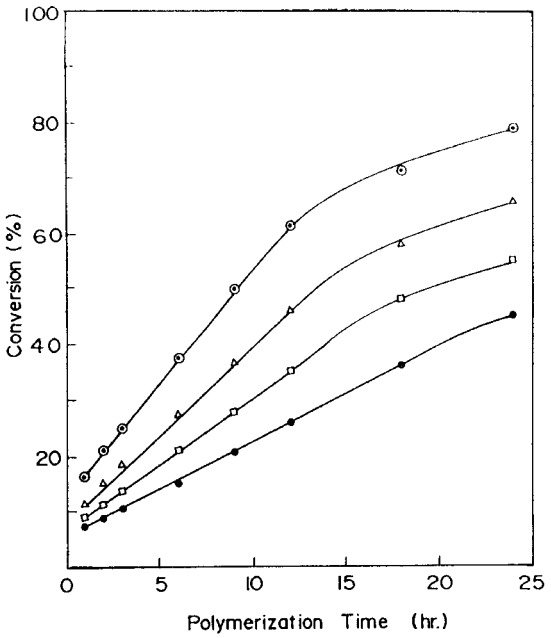

FIG. 1. Time-conversion plots for MMA polymerization with BPT at various temperatures in DMF. (●) 65°C, (□) 70°C, (△) 75°C, (⊙) 80°C; $[MMA]_0$ = 2.0 mol/L, $[BPT]_0$ = 0.02 mol/L.

TABLE 1. "Living" Radical Polymerization of MMA by BPT at 70°C in DMF[a]

No.	Time, hours	Conversion, %	GPC results		
			$\overline{M}_n \times 10^{-3}$	$\overline{M}_w \times 10^{-3}$	$\overline{M}_w/\overline{M}_n$
1	1	9.24	6.73	181.15	26.93
2	2	11.51	8.78	134.46	15.31
3	3	14.02	12.35	125.34	10.15
4	6	21.12	19.33	123.46	6.39
5	9	27.82	25.56	142.66	5.58
6	12	35.23	32.29	163.55	5.07
7	18	47.52	45.05	185.57	4.12
8	24	55.03	62.03	192.46	3.10

[a]$[MMA]_0$ = 2.0 mol/L; $[BPT]_0$ = 0.02 mol/L.

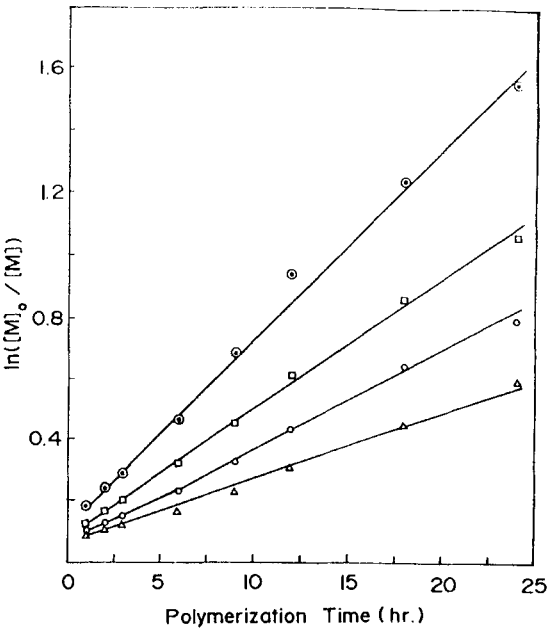

FIG. 2. Time-ln([M]$_0$/[M]) plots for MMA polymerization with BPT at various temperatures in DMF. (△) 65°C, (○) 70°C; (□) 75°C; (⊙) 80°C; [MMA]$_0$ = 2.0 mol/L, [BPT]$_0$ = 0.02 mol/L.

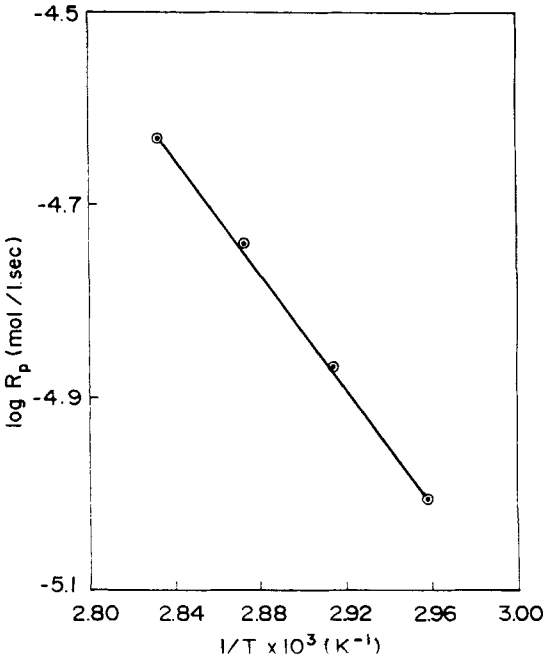

FIG. 3. Arrhenius plot of log R_p vs $1/T$ for MMA polymerization with BPT.

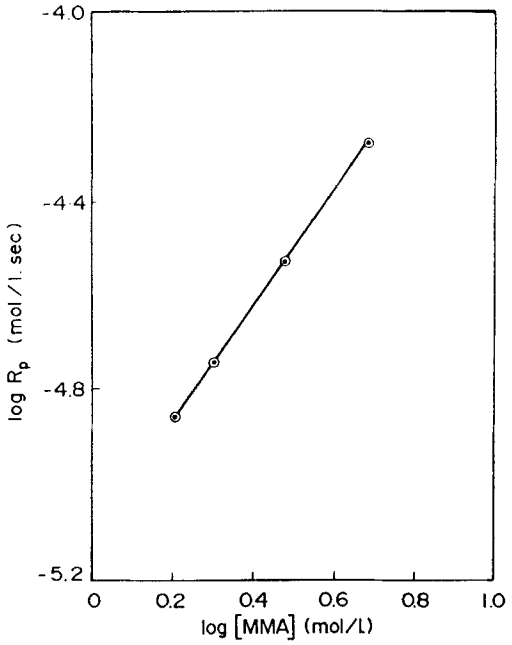

FIG. 4. Plot of log R_p vs log [MMA] for the polymerization of MMA in DMF at 70°C. $[BPT]_0 = 0.02$ mol/L.

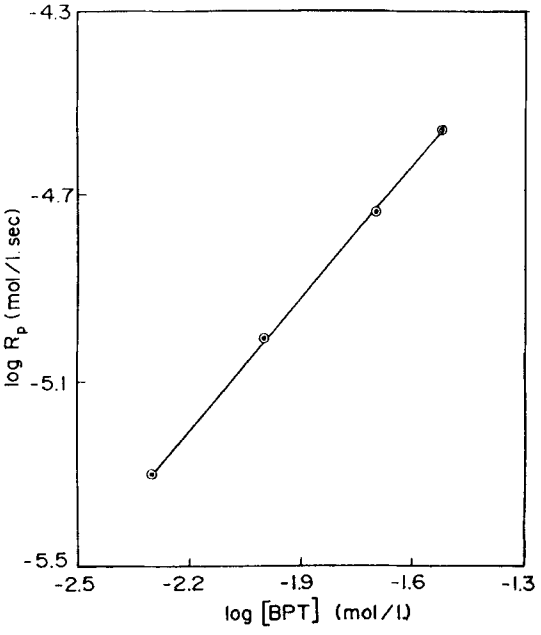

FIG. 5. Plot of log R_p vs log [BPT] for the polymerization of MMA in DMF at 70°C. $[MMA]_0 = 2.0$ mol/L.

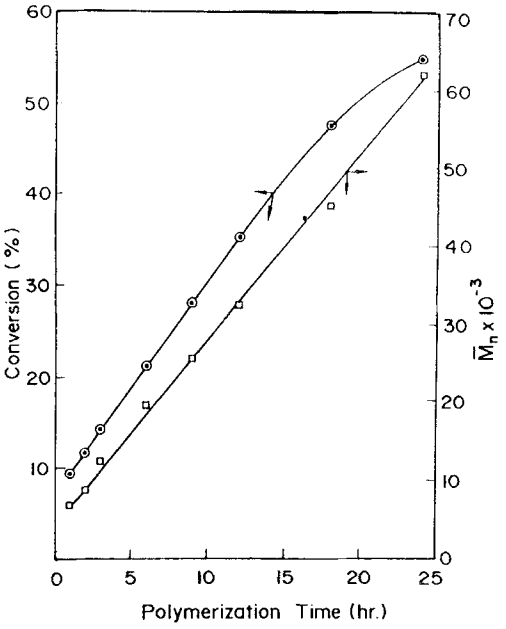

FIG. 6. Time-conversion and time-$\bar{M}_n$ relations for the polymerization of MMA with BPT in DMF at 70°C. $[MMA]_0 = 2.0$ mol/L, $[BPT]_0 = 0.02$ mol/L.

is smaller, a single peak is obtained, whereas if the difference is higher, a bimodal peak is obtained in GPC. Hence, the presence of a single peak in GPC cannot discount the possibility of a "living" radical polymerization mechanism whereas a bimodal distribution pattern clearly substantiates a "living" radical polymerization mechanism.

Figure 7 gives GPC curves for PMMA-BPT at different polymerization times. For comparison, the GPC curve of BPT is also given here at 0 time. Interestingly, bimodal peaks are obtained for PMMA-BPT. It was first believed that the peak corresponding to low molecular weight fractions in Fig. 7 might be due to the presence of residual BPT, but bimodal peaks were obtained even after washing all PMMAs with methanol (BPT is freely soluble in methanol) repeatedly. Hence, it may be inferred that the peak corresponding to low molecular weight fractions in Fig. 7 is not due to the presence of residual BPT but because of low molecular weight fractions of PMMA (A in Eq. 1 and Scheme 2) only. Since the low molecular weight portions are converted into high molecular weight with an increase in polymerization time, the peak corresponding to low molecular weight decreases and simultaneously the peak corresponding to high molecular weight increases. These types of results have been observed [7, 11, 39] in "living" radical polymerization. Hence the present results again confirm that MMA polymerization by BPT proceeds via a "living" radical polymerization mechanism. As the polymerization time increases, the MWD value decreases (Table 1). As the time increases, the MWD is decreased since the bimodal peak tends toward a unimodal peak in GPC.

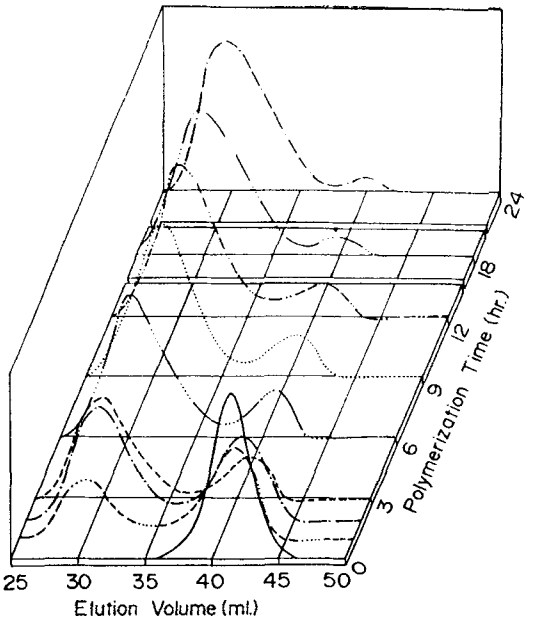

FIG. 7. GPC curves for the polymerization of MMA in DMF at 70°C. $[MMA]_0$ = 2.0 mol/L, $[BPT]_0$ = 0.02 mol/L.

Postpolymerization Studies

The PMMA-PBTs obtained at various polymerization times are considered to have a dormant "living" radical species (i.e., iniferter site) at the chain ends. Hence, these polymers can further be postpolymerized in the presence of the same monomer or another monomer. In Eq. (2), fragment D gives a high molecular weight homopolymer in the presence of the same monomer. If another vinyl monomer (say *y*M) is used, then it is possible to prepare a block copolymer of P and M. In all cases, if the postpolymerization follows "living" radical polymerization, then the yield and molecular weight should increase with respect to time. In order to check this, PMMA-BPT was postpolymerized in the absence and presence of MMA or ST. For all postpolymerization studies, PMMA-BPT prepared (2 mol/L MMA; 0.02 mol/L BPT; 70°C) at 12 hours was used. Interestingly, PMMA-BPT initiates the polymerization of MMA (Table 2) as well as of ST (Table 3). Figure 8 shows time-conversion and time-$\overline{M}_n$ plots for the postpolymerization of PMMA-BPT in the presence and absence of MMA at 70°C in DMF. As the postpolymerization time increased, both yield and $\overline{M}_n$ of PMMA-BPT also increased in the presence of MMA, and $\overline{M}_n$ increased in the absence of MMA. These results show that the dormant PMMA-BPT chains cleave into active species and continue further polymerization. Hence, postpolymerization of PMMA-BPT takes place through a "living" radical polymerization mechanism. Here the rate of increase of molecular weight is higher in the absence of MMA than in the presence of MMA. This can be explained by the fact that in the former case the PMMA radicals are being terminated with other PMMA radicals, thereby the rate of $\overline{M}_n$ increase is higher; in the latter case propagation is through monomer addition and thereby the rate of increase of $\overline{M}_n$ is lower.

TABLE 2. Postpolymerization of PMMA-BPT at 70°C in DMF[a]

No.	Time, hours	In the presence of MMA				In the absence of MMA		
		Yield,[b] %	$\overline{M}_n \times 10^{-3}$	$\overline{M}_w \times 10^{-3}$	$\overline{M}_w/\overline{M}_n$	$\overline{M}_n \times 10^{-3}$	$\overline{M}_w \times 10^{-3}$	$\overline{M}_w/\overline{M}_n$
1	0.0	13.50	32.29	163.55	5.07	32.29	163.55	5.07
2	1.0	15.16	35.54	173.39	4.88	—	—	—
3	4.0	20.44	41.61	178.27	4.28	44.33	175.43	3.96
4	11.0	34.12	53.32	180.83	3.39	65.95	190.10	2.88
5	20.0	39.52	59.64	184.39	3.09	80.81	192.45	2.38
6	36.5	43.24	67.89	188.62	2.78	99.36	194.32	1.96

[a]$[MMA]_0$ = 2.0 mol/L; $[PMMA\text{-}BPT]_0$ = 3.125 g/dL.
[b]Including initial weight of PMMA-BPT.

Figure 9 shows time-conversion and time-$\overline{M}_n$ relations for the block copolymerization of ST with PMMA-BPT in DMF at 70°C. Conversion based on total weight of PMMA-BPT and ST was increased with increasing block copolymerization time. Conversion based on total weight of PMMA-BPT and ST, after extracting homopolymers, was also increased with increasing block copolymerization time. The percentage of block copolymer present in the crude product also increased with increasing block copolymerization time. After removal of homopolymers, $\overline{M}_n$ of the block copolymer increased with increasing block copolymerization time. Thus block copolymerization of PMMA-BPT with ST follows a "living" radical polymerization. Figure 10 gives conversion-$\overline{M}_n$ plots for the chain extension of PMMA-BPT in the presence of MMA and ST. As the conversion increases, $\overline{M}_n$ also in-

TABLE 3. Block Copolymerization of ST with PMMA-BPT at 70°C in DMF[a]

No.	Time, hours	Conversion, %			GPC results[b]		
		Q[c]	R[d]	S[e]	$\overline{M}_n \times 10^{-3}$	$\overline{M}_w \times 10^{-3}$	$\overline{M}_w/\overline{M}_n$
1	0	13.05	—	—	32.29	163.55	5.07
2	3	14.24	1.49	10.44	49.15	153.11	3.12
3	6	16.35	3.13	19.12	54.24	130.49	2.41
4	12	20.34	5.91	29.06	57.99	130.65	2.25
5	24	28.18	11.57	41.06	62.68	130.82	2.09

[a]$[ST]_0$ = 2.0 mol/L; $[PMMA\text{-}BPT]_0$ = 3.125 g/dL.
[b]After extraction of homopolymers, using acetonitrile and cyclohexane.
[c]Based on the total weight of ST and PMMA-BPT.
[d]Based on the total weight of ST and PMMA-BPT after extraction of homopolymers.
[e]Percentage of block copolymer (after extraction of homopolymers) present in the crude product.

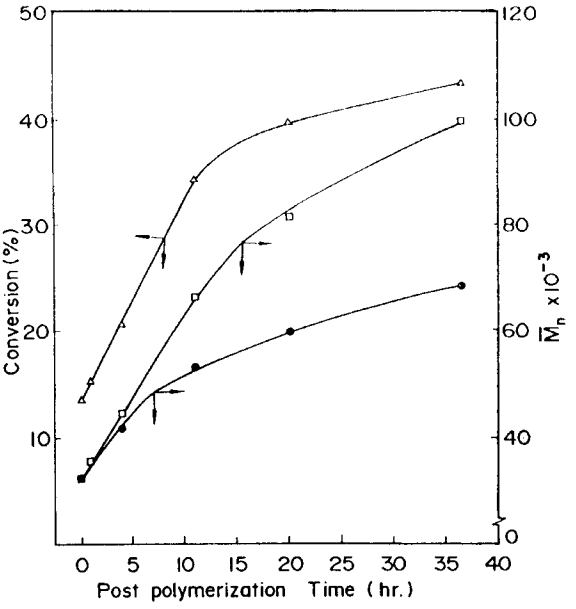

FIG. 8. Postpolymerization of PMMA-BPT at 70°C in DMF. Time-conversion and time-$\bar{M}_n$ relations in the presence of MMA (Δ, ●), and time-$\bar{M}_n$ relation in the absence of monomers (□). $[MMA]_0$ = 2.0 mol/L, $[PMMA\text{-}BPT]_0$ = 3.125 g/dL.

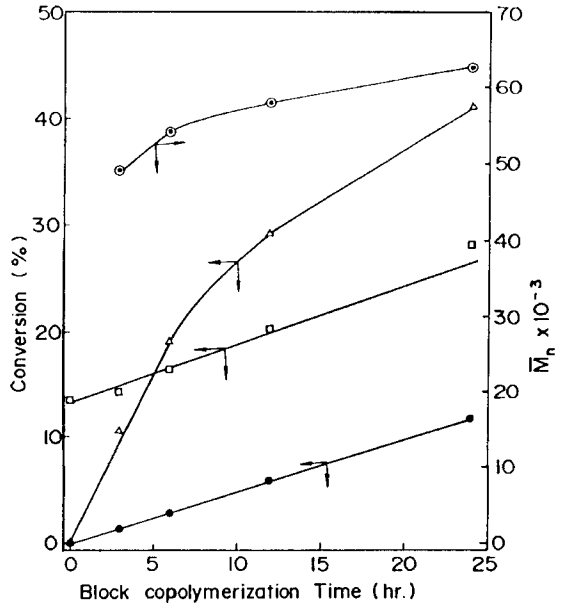

FIG. 9. Time-conversion and time-$\bar{M}_n$ (⊙) relations for the block copolymerization of ST with PMMA-BPT at 70°C in DMF. Conversion based on total weight of PMMA-BPT and ST before extraction (□) and after extraction (●). Percentage of block copolymer present after extraction of homopolymers from the crude product (Δ). $[PMMA\text{-}BPT]_0$ = 3.125 g/dL, $[ST]_0$ = 2.0 mol/L.

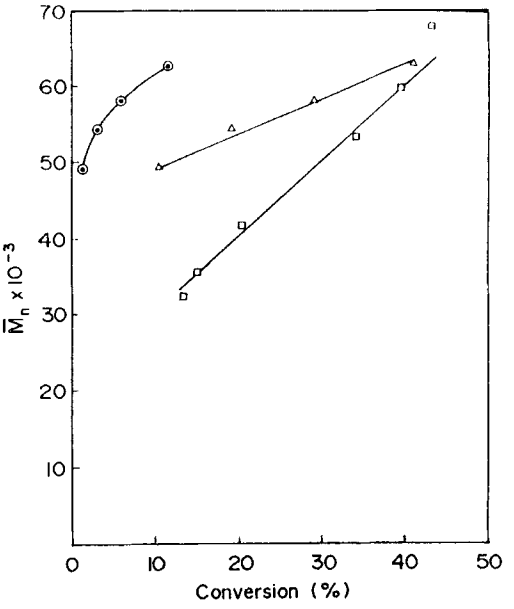

FIG. 10. Conversion-$\bar{M}_n$ plots for postpolymerization with MMA (□) and block copolymerization with ST by PMMA-BPT at 70°C in DMF (⊙) based on the total weight of PMMA-BPT and ST after extraction; (△) based on the percentage of block copolymer present in the crude product after extraction of homopolymers. $[PMMA\text{-}BPT]_0 = 3.125$ g/dL, $[MMA]_0 = [ST]_0 = 2.0$ mol/L.

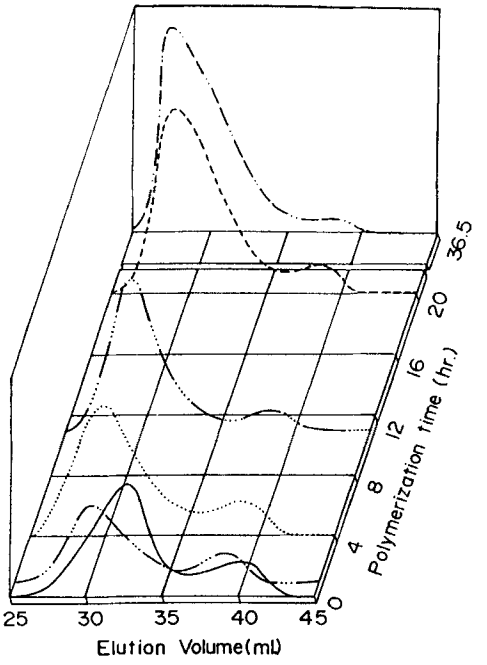

FIG. 11. GPC curves for the postpolymerization of PMMA-BPT with MMA at 70°C in DMF. $[MMA]_0 = 2.0$ mol/L, $[PMMA\text{-}BPT]_0 = 3.125$ g/dL.

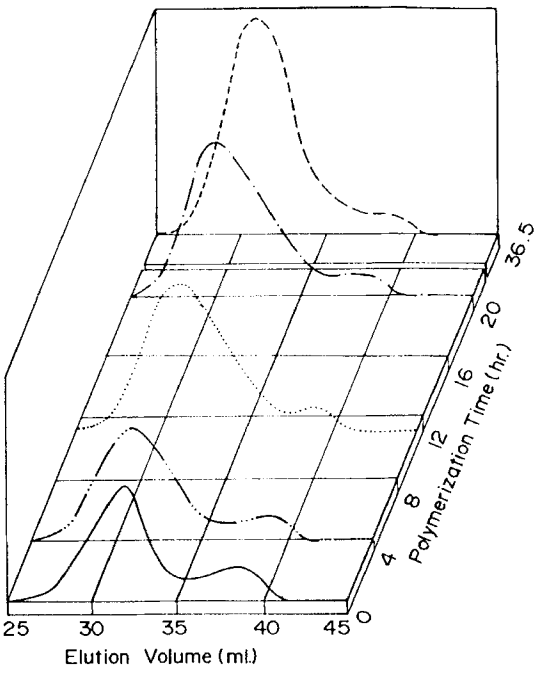

FIG. 12. GPC curves for the postpolymerization of PMMA-BPT in the absence of MMA at 70°C in DMF. $[PMMA\text{-}BPT]_0 = 3.125$ g/dL.

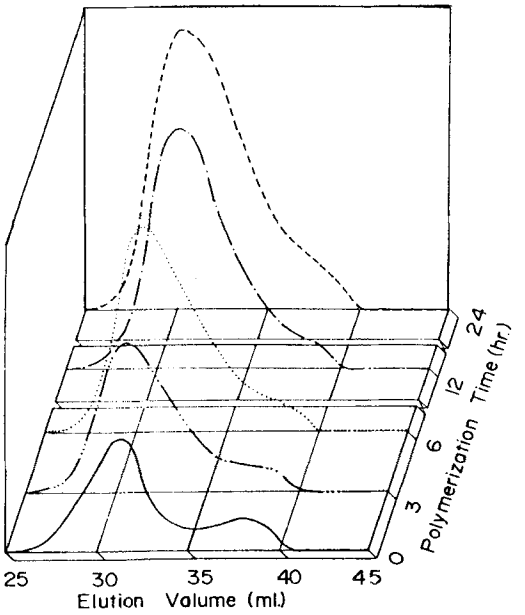

FIG. 13. GPC curves for the block copolymers obtained after extracting homopolymers. $[ST]_0 = 2.0$ mol/L, $[PMMA\text{-}BPT]_0 = 3.125$ g/dL.

creases. Thus postpolymerization of PMMA-BPT in the presence of MMA and ST follows a "living" radical polymerization mechanism. Since the low molecular weight fractions in the postpolymerization of PMMA-BPT in the presence of MMA or ST is higher than in the absence of MMA, the MWD (cf. Tables 2 and 3) of the former case is higher than of the latter case, because the low molecular weight fractions influence the polydispersity significantly. Figures 11, 12, and 13 show GPC curves for the postpolymerization of PMMA-BPT in the presence of MMA, in the absence of monomers and in the presence of ST, respectively, at 70°C in DMF. As in the first stage, the GPC curves of postpolymerization show that when the peaks for low molecular weight fractions are decreased, simultaneously the peaks for high molecular weight fractions are increased in all cases. Hence the postpolymerization of PMMA-BPT in the presence and absence of MMA as well as the block copolymer with ST proceed via a "living" radical polymerization.

After extracting homopolymers by using cyclohexane (for homo-PST) and acetonitrile (for homo-PMMA) from the crude block copolymers, the insoluble portion was completely soluble in DMF and chloroform. This fact eliminates cross-linking and confirms block copolymer formation. Figure 14 shows the ^{1}H-NMR spectrum of the block copolymer (obtained at 24 hours; cf. Table 3), which exhibits signals at 0.80–1.1 ppm (CH_3), 1.3–2.3 ppm (backbone CH_2 and CH), 3.6 ppm ($O-CH_3$), and 6.33–7.1 ppm (phenyl protons). ^{1}H-NMR is an effective tool to determine percentages of PMMA and PST present in the block copolymer. Phenyl ring protons of PST and $O-CH_3$ protons of PMMA are generally used for this purpose. However, in our case, initiator fragments are present in the block copolymer (cf. E in Scheme 2), which could lead to errors in composition. The backbone $-CH$ protons of PST and $-OCH_3$ protons of PMMA can also be used to determine the composition, but since the backbone $-CH$ signal is merged with $-CH_2$ protons of the PST and PMMA, a different approach to quantify block copolymer has been adopted. The integral value of two protons was calculated from the inte-

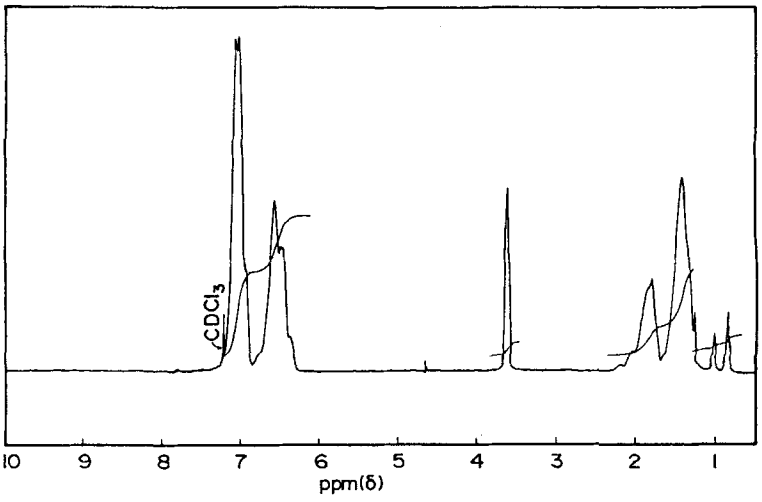

FIG. 14. ^{1}H FT-NMR spectrum of PMMA-PST block copolymer.

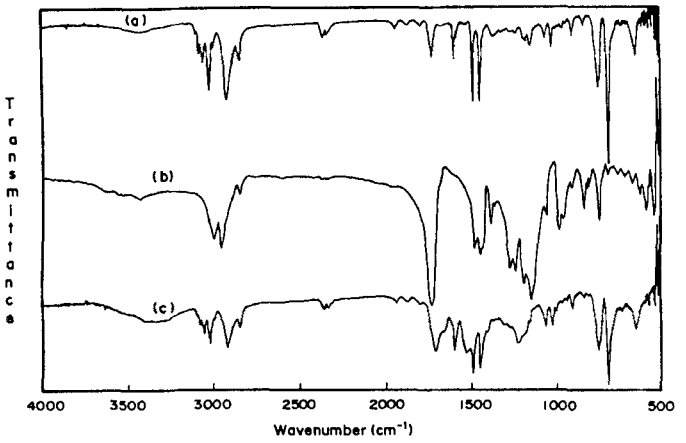

FIG. 15. FT-IR spectra of (a) PST-BPT, (b) PMMA-BPT, and (c) PMMA-PST block copolymers.

gral value of $-O-CH_3$, which was subtracted from the total integral value of $-CH_2$ and $-CH$ protons of both PST and PMMA blocks, leading to the integral value of $-CH_2$ and $-CH$ protons of the PST backbone alone. By comparing the integral values of PST backbone protons and $O-CH_3$ protons, it was determined that 23% PMMA is present in the PMMA-PST block copolymer. The higher percentage (77%) of PST in PMMA-PST block copolymer is probably due to the longer reaction time (24 hours). The block copolymers (obtained at 24 hours; cf. Table 3) were further characterized by FT-IR, DSC, and TGA techniques. The homopolymers PMMA-BPT (prepared at 12 hours; cf. Table 1) and PST (prepared

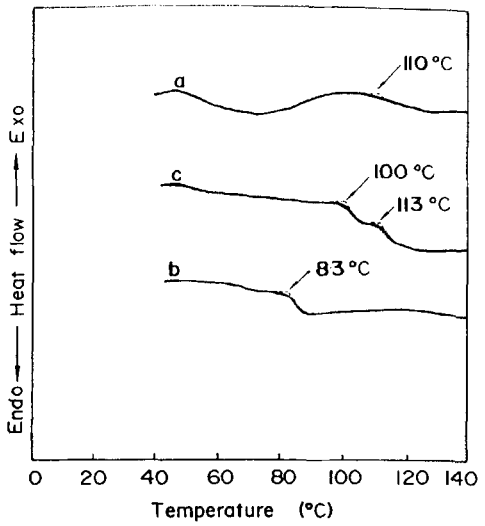

FIG. 16. DSC curves of (a) PMMA-BPT, (b) PST-BPT, and (c) PMMA-PST block copolymers.

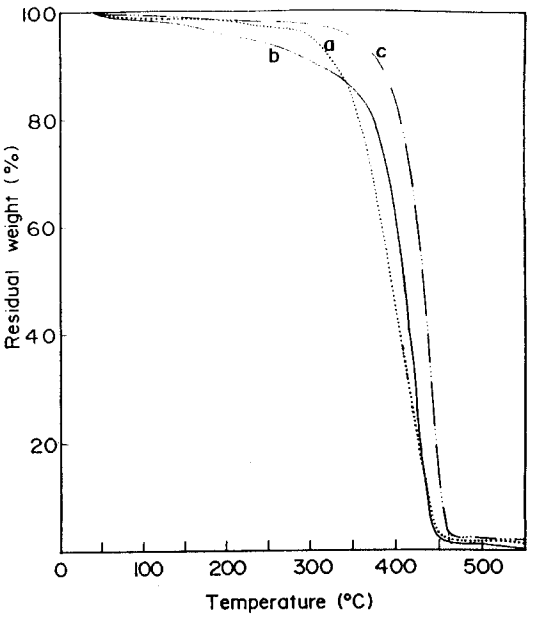

FIG. 17. TGA thermograms of (a) PMMA-BPT, (b) PST-BPT, and (c) PMMA-PST block copolymers.

by a procedure similar to PMMA-BPT from ST and BPT; hereinafter referred to as PST-BPT) were also characterized by the same techniques for comparison. The FT-IR spectra of PMMA-BPT, PST-BPT, and PMMA-PST block copolymer are shown in Fig. 15. The presence of characteristic peaks at 1736 and 3084 to 3029 cm^{-1} correspond to the ester carbonyl of PMMA-BPT and the $-CH$ stretching of the benzene ring present in PST-BPT confirm the formation of block copolymer. In order to find the glass transition temperature (T_g), DSC was used; the curves are presented in Fig. 16. The T_gs of PMMA-BPT, PST-BPT, and PMMA-PST block copolymers appeared at 110, 83, and 100°C as well as 113°C, respectively. Even though the T_gs of PMMA and PST are very close, two T_gs for each of the separate blocks are obtained for the PMMA-PST block copolymer. Figure 17 shows the TGA thermograms of PMMA-BPT, PST-BPT, and PMMA-PST block copolymers. It is interesting to note that the thermal stability of PMMA-PST block copolymer is higher than that of its corresponding homopolymers. The use of polyurethane macroinitiators, which consist of tetraphenylethane groups between polyurethane blocks, to prepare polyurethane-vinyl multiblock copolymers is under investigation.

CONCLUSIONS

Polymethyl methacrylate was synthesized using a novel polyurethane iniferter (BPT). The rate equation for the polymerization of MMA with BPT in DMF was

obtained as $R_p = k[BPT]^{0.95}[MMA]^{1.2}$. Since BPT has organic moieties between initiating groups, homopolymer was obtained. Both conversion and molecular weight increased with increasing polymerization time. A bimodal peak was obtained in GPC. Increases of molecular weight and conversion were observed when PMMA-BPT was heated in the presence of MMA and ST. The block copolymerization of PMMA-BPT in the presence of ST yielded PMMA-PST block copolymer. Hence it is confirmed that BPT acts as a thermal iniferter and follows "living" radical polymerization.

ACKNOWLEDGMENT

One of the authors, K. T., would like to thank the Council of Scientific Industrial Research (CSIR), New Delhi, India, for financial support.

REFERENCES AND NOTES

[1] T. Otsu and M. Yoshida, *Makromol. Chem., Rapid Commun., 3*, 127 (1982).
[2] T. Otsu, M. Yoshida, and T. Tazaki, *Ibid., 3*, 133 (1982).
[3] T. Otsu, M. Yoshida, and A. Kuriyama, *Polym. Bull., 7*, 45 (1982).
[4] T. Otsu and M. Yoshida, *Ibid., 7*, 197 (1982).
[5] T. Otsu and A. Kuriyama, *Ibid., 11*, 135 (1984).
[6] T. Otsu and A. Kuriyama, *J. Macromol. Sci.—Chem., A21*, 961 (1984).
[7] T. Otsu and T. Tazaki, *Polym. Bull., 16*, 277 (1986).
[8] A. Kuriyama and T. Otsu, *Polym. J., 16*, 511 (1984).
[9] A. Bledzki and D. Braun, *Polym. Bull., 16*, 19 (1986).
[10] T. Tazaki and T. Otsu, *Ibid., 17*, 127 (1987).
[11] T. Otsu, A. Matsumoto, and T. Tazaki, *Ibid., 17*, 323 (1987).
[12] C. P. R. Nair, P. Chaumont, and G. Clouet, *J. Macromol. Sci.—Chem., A27*, 791 (1990).
[13] G. Clouet and D. Kayser, *J. Polym. Sci., Polym. Chem. Ed., 31*, 3387 (1993).
[14] S. I. Kuchanov, *Ibid., 32*, 1557 (1994).
[15] D. Greszta, D. Mardare, and K. Matyjaszewski, *Macromolecules, 27*, 638 (1994).
[16] M. Lee, K. Utsumi, and Y. Minoura, *J. Chem. Soc., Faraday Trans. 1, 75*, 1821 (1979).
[17] D. Mardare and K. Matyjaszewski, *Macromolecules, 27*, 645 (1994).
[18] K. Matyjaszewski, *J. Macromol. Sci.—Pure Appl. Chem., A31*, 989 (1994).
[19] R. P. N. Veregin, M. K. Georges, P. M. Kazmaier, and G. K. Hamer, *Macromolecules, 26*, 5316 (1993).
[20] K. Matyjaszewski, S. Gaynor, and J. S. Wang, *Ibid., 28*, 2093 (1995).
[21] S. Gaynor, D. Greszta, D. Mardare, M. Teodorescu, and K. Matyjaszewski, *J. Macromol. Sci.—Pure Appl. Chem., A31*, 1561 (1994).
[22] T. Otsu, A. Matsumoto, and M. Yoshioka, *Indian J. Technol., 31*, 172 (1993) and references therein.

[23] D. Braun and K. H. Becker, *Makromol. Chem., 147*, 91 (1971).
[24] G. Nijst and G. Smets, *Makromol. Chem., Rapid Commun., 2*, 481 (1981).
[25] J. V. Crivello, D. A. Conlon, and J. L. Lee, *J. Polym. Sci., Polym. Chem. Ed., 24*, 1197 (1986).
[26] J. V. Crivello, J. L. Lee, and D. A. Conlon, *Ibid., 24*, 1251 (1986).
[27] D. Braun and K. H. Becker, *Angew. Makromol. Chem., 6*, 186 (1969).
[28] K. Tharanikkarasu and G. Radhakrishnan, *Eur. Polym. J., 30*, 1351 (1994).
[29] K. Tharanikkarasu and G. Radhakrishnan, *J. Polym. Sci., Polym. Chem. Ed.*, Communicated.
[30] *Vogel's Textbook of Practical Organic Chemistry*, 4th ed., ELBS/Longman, England, 1987, p. 359.
[31] Molecular weight of the repeating unit (540.62) was used for all mole calculations of BPT.
[32] D. C. Neckers and D. P. Colenbrander, *Tetrahedron Lett., 48*, 5045 (1968).
[33] A. Bledzki, D. Braun, and K. Titzschkau, *Makromol. Chem., 184*, 745 (1983).
[34] A. Bledzki, D. Braun, W. Menzel, and K. Titzschkau, *Ibid., 184*, 287 (1983).
[35] L. M. Arnett, *J. Am. Chem. Soc., 74*, 2027 (1952).
[36] E. Borsig, M. Lazar, and M. Capla, *Makromol. Chem., 105*, 212 (1967).
[37] S. R. Turner and R. W. Blevins, *Macromolecules, 23*, 1856 (1990).
[38] K. Endo, K. Murata, and T. Otsu, *Ibid., 25*, 5554 (1992).
[39] Z. Liu, D. Yan, and J. Shen, *Makromol. Chem., Rapid Commun., 9*, 27 (1988).

Received June 13, 1995
Revision received August 28, 1995